Photovoltaic study of ZnSe/GaAs heterostructures

J. B. Wang, D. Y. Chen, C. X. Jin, F. Lu, H. H. Sun, and X. Wang
Surface Physics Laboratory and T. D. Lee Physics Laboratory, Fudan University, Shanghai, 200433, China
(Received 3 October 1996)

The ZnSe/GaAs heterojunctions formed by epitaxially grown ZnSe thin films on *S*-treated GaAs substrates are characterized by the photovoltaic measurements. By analyzing the photovoltaic spectra obtained at different temperatures, the broad-band photovoltaic signal is assigned to the cross-band photon-absorption transitions between the valence band of GaAs and the conduction band of ZnSe near the heterointerface. The band alignment of the ZnSe/*S*-GaAs heterojunction is determined to be of a type-II configuration with a conduction-band offset of 168 meV at room temperature. [S0163-1829(97)00924-7]

I. INTRODUCTION

Recently, the investigation of the physical properties of ZnSe-based II-VI wide-band-gap semiconductors has attracted much attention due to their important potential applications in optoelectronics. With a small-lattice mismatch of about 0.27% at room temperature, ZnSe/GaAs heterostructures of high quality could be readily achieved by epitaxial-growth techniques, and have been studied intensively.[1–4] However, due to the complexity of the buried heterovalent interfaces which are difficult to be probed, a discrepancy is exhibited among the experimental results of the conduction- and valence-band discontinuities. Using Raman scattering measurements, Olego[5] found that the ZnSe/GaAs heterojunction has a type-I band alignment with a conduction-band offset of 0.3 eV, which was confirmed by the electrolyte-electroreflectance measurement performed by Kassel *et al.*[6] Han *et al.*[7] obtained a different result by the measurement of transverse acoustoelectric voltage spectroscopy, from which the band alignment is revealed to be of type-II with a conduction-band offset of 0.059 eV. Nicolini *et al.*[8] have related the band offsets with the atomic structure and composition of the interface and showed that the detail of the sample fabrication plays a crucial role in determining the band discontinuities at the heterointerface.

In this work, the photovoltaic (PV) measurement is used to study the ZnSe/GaAs heterojunctions prepared with sulfur-passivation treatments prior to the epitaxial growth. It is found that a broad-band PV signal is observed for the heterojunctions treated with sulfur passivation. A theoretical calculation, which takes into account the photovoltages yielded by both the carriers swept out of the space-charge region and those accumulated in the triangle wells at the interface, is carried out to fit the experimental PV spectra. The results show that the PV spectra are originated by the crossband transition from the valence band of GaAs to the conduction band of ZnSe with a type-II band lineup at the heterointerface. The rationality of the analysis is corroborated by the current-voltage measurement.

II. EXPERIMENT

Samples used in the PV measurements were grown by the molecular beam epitaxy (MBE) on n^+-GaAs(100) wafers with a doping concentration of 1×10^{17} cm^{-3}. After the pregrowth chemical cleaning, the GaAs substrates were treated with sulfur passivation in order to improve the quality of the epitaxial heterointerface.[9] After being loaded into the MBE chamber, the substrate was heated to 380 °C for 10 min to remove the extra sulfur on the surface and then cooled down to 280 °C to carry out the growth. Three samples were prepared. Samples S1 and S2 were treated with S_2Cl_2 and $(NH_4)_xS$ passivations before growth, respectively. For comparison, sample S3 is a GaAs substrate treated with S_2Cl_2 passivation and exposed to Se beam flux for 1 min without growing the ZnSe epitaxial layer. The unintentionally-doped ZnSe epitaxial layers were found to be *n*-type with a doping concentration of about 1×10^{16} cm^{-3}. The thicknesses of the samples are about 100 nm which is smaller than the critical thickness for pseudomorphic growth, so the heterointerfaces are expected to be free of misfit dislocations.

To carry out the PV measurement, a Schottky contact with an area of about 5×10^{-3} cm^2 was made on the front side of the sample by evaporating Al through a mask. An ohmic contact was formed by alloying indium on the back side. The sample was mounted on the cold head of a close-cycle helium refrigerator, its temperature could vary in the range of 18–300 K. The PV spectra were measured under the illumination of a monochromatic-light dispersed from a halogen tungsten lamp and chopped at a frequency of about 70 Hz. The photovoltaic signal was detected by a lock-in amplifier. The energy resolution of the instrument is about 3 meV.

III. RESULTS AND DISCUSSION

In Fig. 1, the dots are the PV spectra taken at room temperature. The spectra of samples S1 and S2 show a broad-band peaked at 1.3 eV below the steep rise of the intensity which is originated from the band-edge absorption of GaAs. It could be seen more clearly in Fig. 2, which shows the PV spectra of sample S1 measured at low temperatures. To make a comparison, the PV spectrum of sample S3 of a GaAs substrate without the ZnSe epitaxial layer, was taken at room temperature and also shown in Fig. 1, in which no broad band is observed. This implies that the broad band is not related to any absorption-transition processes in the substrate

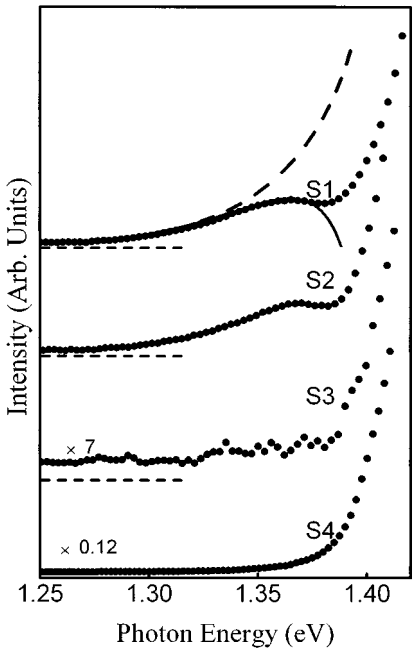

FIG. 1. The photovoltaic spectra of samples S1 and S2 taken at room temperature. S1 and S2 are ZnSe/GaAs samples, S3 is a GaAs substrate. The dashed curve and the solid curve are the line shapes derived from Eq. (2) and Eq. (7), respectively.

stimulated by photons with an energy smaller than the band gap of GaAs. It could also be excluded that the broad band is related to the transitions between the localized-deep level in the band gap of ZnSe, if existed, and the conduction-or valence-band of ZnSe, since these transitions possess the well-known line shape of a peak with a long tail at the high-energy side rather than a broad band like those of samples S1 and S2 with a long tail at the low-energy side. The transitions between two localized deep levels could be plausibly ruled out in that, contrary to the results shown in Fig. 2, the PV signal of these transitions must increase dramatically as the temperature ascends because the excited electrons or holes need to be excited thermally further to the conduction- or valence-band to yield the PV signal. Excluding the above possibilities, the origin of the broad band would be unambiguously attributed to the heterointerface.

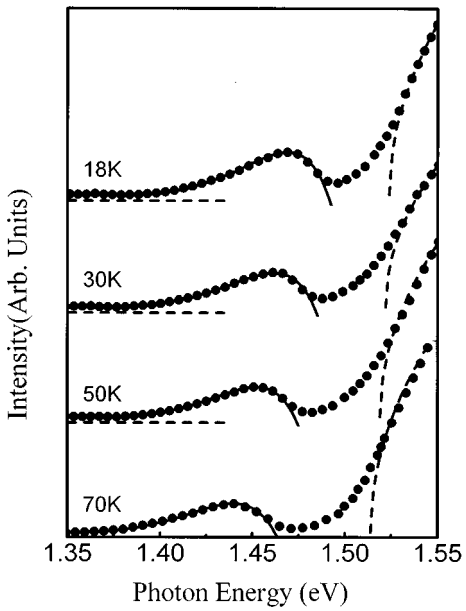

FIG. 2. The photovoltaic spectra of sample S1 at different temperatures. The solid and dashed curves are the theoretical line shapes derived from Eqs. (7) and (8), respectively.

If there exist interfacial states with energy levels in the band gap of GaAs, the following possible transitions would be expected to occur at the heterointerface: (a) transition from the interfacial state(s) to the conduction band of ZnSe; (b) transition from the interfacial state(s) to the conduction band of GaAs; (c) transition from the valence band of GaAs to the interfacial state(s); (d) transition from the interfacial state(s) near the valence band of GaAs to that near the conduction band of GaAs; (e) transition from the valence band of GaAs to the conduction band of ZnSe provided that the conduction-band minimum of ZnSe is below that of GaAs, i.e., the band lineup is of a type-II configuration. However, possibilities (a)–(d), which should have almost the same temperature effect as that of band gaps, could be ruled out based on the peak position shifting at low temperatures. From Fig. 2 it could be seen that the peak position shifts from 1.47 eV at 18 K to 1.44 eV at 70 K, which is much larger than the shifts of the band gaps of GaAs and ZnSe caused by the temperature effect, both of which are about 0.01 eV in that temperature range. Thus, the only possibility which is responsible to the PV spectra is the case (e). It means that the ZnSe/GaAs heterointerface of our sample has a type-II band alignment and the PV broad-band structure is resulted from the cross-band transitions between the valence band of GaAs and the conduction band of ZnSe which are shown schematically in Fig. 3.

The rationality of the above assumption is checked by a theoretical calculation of the line shape of the cross-band transitions. Assuming that the wave functions for the αth state of the valence band of GaAs and the βth state of conduction band of ZnSe are $\psi_{V\alpha}(z)$ and $\psi_{C\beta}(z)$, respectively. The transition probability between these two states, $P_{\alpha\beta}$, can be expressed as

$$P_{\alpha\beta} \propto \left| \int_{-\infty}^{+\infty} \psi_{C\beta}(z)^* \psi_{V\alpha}(z) dz \right|^2 \delta(\hbar\omega + E_\alpha - E_\beta). \quad (1)$$

Due to the large valence-band offset and relatively small conduction-band offset between ZnSe and GaAs, $\psi_{V\alpha}(z)$ vanishes in the ZnSe region ($z<0$) whereas $\psi_{C\beta}(z)$ is nonzero in the GaAs region ($z>0$), resulting in the overlap of wave functions in the GaAs region near the interface, thus, $P_{\alpha\beta}$ is not vanished. By summing up all the states in the conduction and valence bands that are possibly involved in the transitions, the transition probability $G(\omega)$ after the sample is illuminated by photons with an energy of $\hbar\omega$ is derived from Eq. (1) to be (see the Appendix):

$$G(\omega) = C\left[\arcsin\left(\frac{\hbar\omega - E_g + \Delta_C}{\Delta_C} \right) - \frac{\hbar\omega - E_g + \Delta_C}{\Delta_C} \right] \quad \text{for } \hbar\omega < E_g, \quad (2)$$

where E_g is the band gap of GaAs, Δ_C is the conduction-band offset between GaAs and ZnSe, and C is a constant

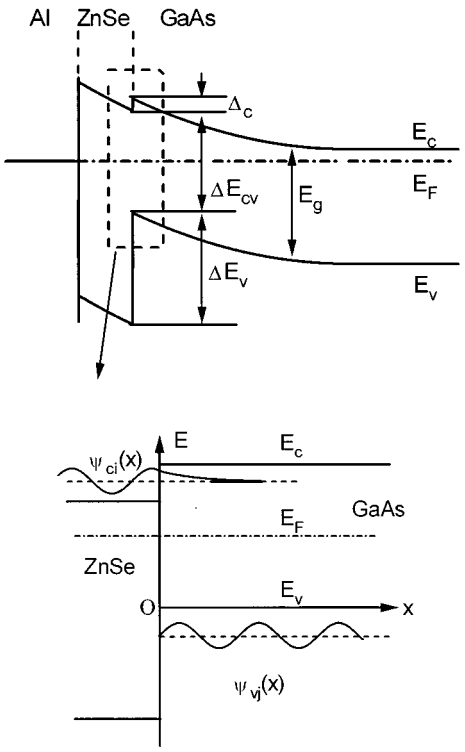

FIG. 3. Schematic-band diagrams of the ZnSe/GaAs heterostructure.

which is independent of $\hbar\omega - E_g$ and Δ_C. The best fit of Eq. (2) to the experimental spectrum is shown as the dashed curve in Fig. 1 by suitably adjusting the parameters C, E_g, and Δ_C. It shows good coincidence only at the low-energy side. The cause of the deviation could be attributed to the band-discontinuity structure of the heterojunction. From the band diagram shown in Fig. 3, it is obvious that all the photogenerated holes would accumulate in the triangle well of the valence bands near the interface due to the large-band discontinuity between the valence bands. While in the conduction band, the electrons accumulated in the triangle well in the ZnSe side may have the probability of penetrating through and leaping over the barrier into the GaAs side, giving rise to an equivalent current I_1, which is evidently proportional to the areal electron density σ_e, or $G(\omega)\tau$, where τ is the lifetime of the carriers. Thus the photovoltage related with I_1 can be expressed as

$$V_1 = \frac{kT}{e} \ln[aG(\omega) + 1], \tag{3}$$

where k is the Boltzmann constant, e is the electron charge, a is a coefficient which is proportional to τ, and the reciprocal of the saturation leakage current $I_0(T)$,

$$a \propto \tau / I_0(T). \tag{4}$$

Moreover, in addition to the above photovoltage V_1 resulting from the space-charge region, the electrons and holes accumulated in the two triangle wells can also yield a photovoltage V_2, which is also proportional to the areal electron density σ_e and can be expressed as

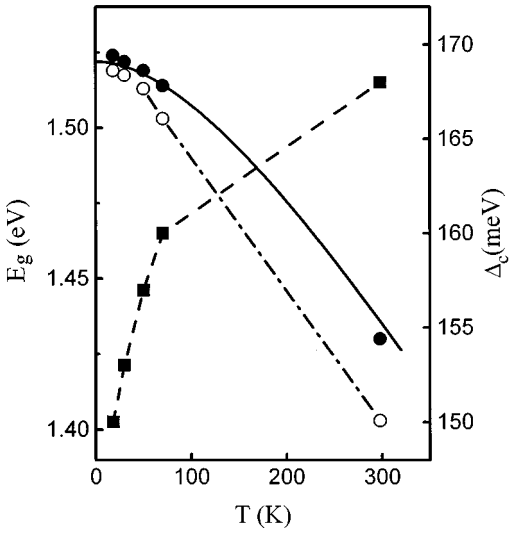

FIG. 4. The band gap of GaAs (E_g), and the conduction-band offset (Δ_C) vs. the temperature. (●) E_g derived from Eq. (7), (○) E_g derived from Eq. (8), (■) Δ_C.

$$V_2 = bG(\omega), \tag{5}$$

where the coefficient b depends on the mean spatial separation between electrons and holes at the interface, and is also proportional to τ.

$$b \propto \tau. \tag{6}$$

Since the polarity of V_2 is opposite to V_1, the total photovoltage is given by

$$V = V_1 - V_2 = \frac{kT}{e} \ln[aG(\omega) + 1] - bG(\omega). \tag{7}$$

By adjusting a, b, Δ_C, and E_g, the PV spectra of sample S1 in Figs. 1 and 2 can be fitted satisfactorily by Eq. (7) as shown by the solid curves there. The dashed curves in Fig. 2 are the well-known square-root absorption line shapes of GaAs,

$$\alpha(\omega) \propto \sqrt{\hbar\omega - E_g}, \tag{8}$$

from which the band gap E_g of GaAs can be obtained as well. The values of Δ_C and E_g as a function of temperature derived from Eqs. (7) and (8) are shown in Fig. 4. The solid curve in Fig. 4 is the theoretical E_g-T relation, which is in good agreement with Eq. (8). The data obtained from Eq. (7) are slightly smaller in the order of kT than those obtained from Eq. (8). This might be due to the fact that it is easier for the hot electrons in the triangle well to leap over the barrier at the interface, resulting in the apparent reduction of the barrier height. From Fig. 4, it could be found that the conduction-band offset Δ_C increases monotonically with the temperature, demonstrating that the temperature dependencies on the conduction bands of GaAs and ZnSe are different.

Due to the lack of theoretical and experimental understanding of the τ-T relation, the parameters a and b cannot serve as proof of the rationality of our analysis. However, from Eqs. (4), and (6), it could be found that the ratio b/a is proportional to the saturating leakage current $I_0(T)$, i.e.,

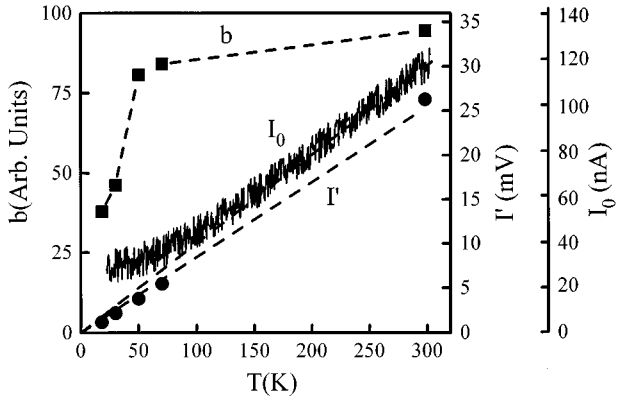

FIG. 5. The saturating leakage current I_0, the parameters Γ (dots) and b (squares) as a function of temperature.

$$\Gamma = b/a \propto I_0(T), \tag{9}$$

which can be obtained by the current-voltage measurement. To carry out the measurement of $I_0(T)$, a small reverse bias of 30 mV was applied. The results of $I_0(T)$ and Γ are shown in Fig. 5, from which the validity of Eq. (9) is verified, demonstrating the reasonableness of our analysis. It could also be seen from Fig. 5 that b, or the carrier lifetime τ at the heterointerface, changes slightly with T within the temperature range of 18–300 K. This might be a result of the Fermi-level pinning at the interfacial states so that the recombination effect on the surplus carriers is basically unchanged with temperature. Moreover, the linear relationship between I_0 and T implies that the carrier transportation in this heterostructure is mainly not the mechanism of thermal emission, the latter should possess an exponential characteristic. To clarify the carrier-transportation mechanism of our samples, further study is needed.

We also did the measurements on several ZnSe/GaAs samples without the S treatment of the GaAs substrates prior to the growth. No broad-band peaked at 1.37 eV was observed, which implies that the interfacial structure is different from that of the passivated one. This is not unreasonable since the structure at the heterointerface depends sensitively on the interfacial atomic arrangement and composition.

IV. SUMMARY

In conclusion, the PV measurements on the ZnSe/GaAs heterojunctions have been carried out in the temperature range of 18–300 K. For the ZnSe grown on S-treated GaAs substrate, a broad band which appeared near the absorption edge of GaAs is observed, which is assigned to the cross-band transitions from the valence band of GaAs to the conduction band of ZnSe. The experimental PV spectra could fit the theoretical derivation only if we assume that the band lineup at the ZnSe/S-GaAs heterointerface is a type-II structure, i.e., the conduction-band edge of ZnSe is lower than that of GaAs with a band offset of 168 meV at room temperature and smaller at lower temperatures. The validity of the analysis is also demonstrated by the results of current-voltage measurements.

ACKNOWLEDGMENT

The authors would like to thank S. K. Zhang for his assistance in this work.

APPENDIX

1. Expressions of the envelope-wave functions

To simplify the discussion, all the effective masses (electron and hole) of ZnSe and GaAs are assumed to be m. The Hamiltonians of the electron and hole could be written as

$$\left[-\frac{\hbar^2}{2m}\frac{d^2}{dz^2}+V(z)\right]\psi(z)=E\psi(z), \tag{A1}$$

where $V(z)$ is the potential function, $\psi(z)$ is the envelope wave function, and E is the energy. For the electron,

$$V(z)=\begin{cases} E_{CV}, & z<0 \\ E_{CV}+\Delta_C, & z>0. \end{cases} \tag{A2}$$

Thus, the envelope wave function $\psi_{C\beta}(z)$ of the βth electron state with an energy of $E_\beta = E_{CV}+(\hbar^2 k_\beta^2/2m)$ could be derived as

$$\psi_{C\beta}(z) = \begin{cases} \frac{1}{2}\left(1+i\frac{K_\beta}{k_\beta}\right)Ce^{ik_\beta z}+\frac{1}{2}\left(1-i\frac{K_\beta}{k_\beta}\right)Ce^{-ik_\beta z}, & z<0 \\ Ce^{-K_\beta z}, & z>0, \end{cases} \tag{A3}$$

where

$$K_\beta^2+k_\beta^2=\frac{2m}{\hbar^2}\Delta_C, \tag{A4}$$

and

$$C=\frac{2\hbar k_B}{\sqrt{2m\Delta_C}}\propto\frac{k_\beta}{\sqrt{\Delta_C}}. \tag{A5}$$

In fact, the βth electron state should have two more quantum numbers $k_{\beta x}$ and $k_{\beta y}$, or $\mathbf{k}_{\beta\perp}$, therefore, the real wave function of the βth electron state could be approximately written as

$$\phi_{C\beta}(\mathbf{r})=g w_{C\beta}(z)e^{i\mathbf{k}_{\beta\perp}\cdot\mathbf{r}}u_{C0}(\mathbf{r}), \tag{A6}$$

where $u_{C0}(\mathbf{r})$ is the Bloch wave function at the Γ-point of the conduction band. Accordingly, the energy of the βth state is

$$E_\beta = E_{CV}+\frac{\hbar^2}{2m}(k_\beta^2+\mathbf{k}_{\beta\perp}^2). \tag{A7}$$

As for the hole state, the envelope function $\psi_{V\alpha}(z)$ of the αth state vanishes for $z<0$ due to the relatively large valence-band offset Δ_V, thus $\psi_{V\alpha}(z)$ could be expressed as

$$\psi_{V\alpha}(z)=\begin{cases} 0, & z<0 \\ \sin k_\alpha z, & z>0. \end{cases} \tag{A8}$$

Just like what was discussed for the βth electron state, the real wave function and the energy of the αth hole state could be found as

$$\phi_{V\alpha}(\mathbf{r}) \approx \psi_{V\alpha}(z) e^{i\mathbf{k}_{\alpha\perp}\cdot\mathbf{r}} u_{V0}(\mathbf{r}), \tag{A9}$$

and

$$E_\alpha = -\frac{\hbar^2}{2m}(k_\alpha^2 + k_{\alpha\perp}^2), \tag{A10}$$

respectively, where $u_{V0}(\mathbf{r})$ is the Bloch wave function at Γ-point of the valence band.

2. Calculation of transition probability

According to Lippmann-Schwinger formula, the probability $P_{\alpha\beta}$ of transition from the αth state of the valence band to the βth state of the conduction band induced by the photon with an energy of $\hbar\omega$ can be written as

$$P_{\alpha\beta} \propto |T_{\alpha\beta}|^2 \delta(\hbar\omega + E_\alpha - E_\beta), \tag{A11}$$

where $\delta(\hbar\omega + E_\alpha - E_\beta)$ is the Dirac delta function,

$$\begin{aligned} T_{\alpha\beta} &\propto \mathbf{A}\cdot\mathbf{P}_{CV}(0)\,\delta_{\mathbf{k}_{\alpha\perp},\mathbf{k}_{\beta\perp}} \int_0^\infty dz\, \frac{k_\beta}{\sqrt{\Delta_C}}\, e^{-K_\beta z} \sin k_\alpha z \\ &= \mathbf{A}\cdot\mathbf{P}_{CV}(0)\, \frac{k_\alpha k_\beta \delta_{\mathbf{k}_{\alpha\perp}\cdot\mathbf{k}_{\beta\perp}}}{\sqrt{\Delta_C}(K_\beta^2 + k_\alpha^2)}, \end{aligned} \tag{A12}$$

and

$$\mathbf{P}_{CV}(0) = \int d\tau u_{C0}(\mathbf{r})^* \mathbf{P} u_{V0}(\mathbf{r}), \tag{A13}$$

which is the matrix element of momentum $\mathbf{P}$. Here $\mathbf{A}$ is the vector potential of the photon field. With the unimportant coefficients omitted, the transition probability stimulated by the photon field with an energy of $\hbar\omega$ can be obtained by summing up $P_{\alpha\beta}$ with all the states that could be involved in the transitions as

$$\begin{aligned} G(\omega) \propto \int d\mathbf{k}_{\alpha\perp} dk_\alpha dk_\beta \frac{1}{\Delta_C} \frac{k_\alpha^2 k_\beta^2}{(K_\beta^2 + k_\alpha^2)^2} \\ \times \delta\left[\hbar\omega - E_{CV} - \frac{\hbar^2}{2m}(k_\alpha^2 + k_\beta^2 + 2\mathbf{k}_{\alpha\perp}^2)\right]. \end{aligned} \tag{A14}$$

According to the definition of the delta function, $G(\omega)$ could be transformed into

$$G(\omega) \propto \frac{1}{\Delta_C} \int_{\hbar^2/2m(k_\alpha^2 + k_\beta^2) \le \hbar\omega - E_{CV}} dk_\alpha dk_\beta \frac{k_\alpha^2 k_\beta^2}{(K_\beta^2 + k_\alpha^2)^2}, \tag{A15}$$

from which it could be found that the integral is taken within a circle with the radius of $\sqrt{(2m/\hbar)(\hbar\omega - E_{CV})}$ in the $k_\alpha k_\beta$ plane. Using the following substitutions:

$$r = \sqrt{(2m/\hbar^2)(\hbar\omega - E_{CV})} = \sqrt{(2m/\hbar^2)(\hbar\omega - E_g + \Delta_C)} = \sqrt{a}, \tag{A16}$$

$$k_\alpha = \rho\, \cos\theta, \tag{A17}$$

$$k_\beta = \rho\, \sin\theta, \tag{A18}$$

and

$$b = \frac{2m}{\hbar^2}\Delta_C, \tag{A19}$$

$G(\omega)$ can be rewritten as

$$\begin{aligned} G(\omega) &\propto \frac{1}{\Delta_C} \int_0^r \rho d\rho \int_0^{2\pi} d\theta\, \frac{\rho^4 \cos^2\theta \sin^2\theta}{(b - \rho^2\cos^2\theta + \rho^2\sin^2\theta)^2} \\ &\propto \frac{1}{\Delta_C} \int_0^a dt \int_0^{2\pi} d\theta\, \frac{t^2 \sin^2\theta}{(b - t\cos\theta)^2}. \end{aligned} \tag{A20}$$

The integration with respect to θ can be transformed as follows:

$$\begin{aligned} \int_0^{2\pi} d\theta\, \frac{t^2\sin^2\theta}{(b - t\cos\theta)^2} &= -\int_0^{2\pi} t\, \sin\theta d\left(\frac{1}{b - t\cos\theta}\right) \\ &= -\frac{t\sin\theta}{b - t\cos\theta}\bigg|_0^{2\pi} + \int_0^{2\pi} \frac{t\cos\theta}{b - t\cos\theta} d\theta \\ &= b\int_0^{2\pi} \frac{d\theta}{b - t\cos\theta} - 2\pi. \end{aligned} \tag{A21}$$

Let $z = e^{i\theta}$, therefore,

$$\begin{aligned} \int_0^{2\pi} \frac{d\theta}{b - t\cos\theta} &= \frac{1}{i} \oint_{|z|=1} \frac{2dz}{2bz - tz^2 - t} \\ &= 2\pi \operatorname*{Res}_{|z|\le 1}\left(\frac{2}{2bz - tz^2 - t}\right), \end{aligned} \tag{A22}$$

where $\mathrm{Res}_{|z|\le 1}[f(z)]$ denotes the residue of $f(z)$ in the region $|z| \le 1$, and could be obtained as

$$\operatorname*{Res}_{|z|\le 1}\left(\frac{2}{2bz - tz^2 - t}\right) = \frac{1}{\sqrt{b^2 - t^2}}. \tag{A23}$$

Thus Eq. (A19) could be rewritten as

$$\begin{aligned} G(\omega) &\propto \frac{1}{\Delta_C}\int_0^a dt\, \frac{2\pi b}{\sqrt{b^2 - t^2}} - \frac{2\pi a}{\Delta_C} \propto \frac{b}{\Delta_C} \arcsin\left(\frac{t}{b}\right)\bigg|_0^a - \frac{a}{\Delta_C} \\ &\propto \arcsin\left(\frac{\hbar\omega - E_g + \Delta_C}{\Delta_C}\right) - \frac{\hbar\omega - E_g + \Delta_C}{\Delta_C}. \end{aligned} \tag{A24}$$

Equation (2) in the text is derived.

[1] N. Kobayashi, Appl. Phys. Lett. **55**, 1235 (1989).
[2] D. Li, J. M. Gonsalves, N. Otsuka, J. Qiu, M. Kobayashi, and R. L. Gunshor, Appl. Phys. Lett. **57**, 449 (1990).
[3] M. S. Yeganeh, J. Qi, and A. G. Yodh, M. C. Tamargo, Phys. Rev. Lett. **68**, 3761 (1992).
[4] Z. Yang, G. K. Wong, I. K. Sou, and Y. H. Yeung, Appl. Phys. Lett. **66**, 2235 (1995).
[5] D. J. Olego, Phys. Rev. B **39**, 1 2743 (1989).
[6] L. Kassel, H. Abad, J. W. Garland, P. M. Raccah, J. E. Potts, M. A. Haase, and H. Cheng, Appl. Phys. Lett. **56**, 42 (1990).
[7] K. J. Han, A. Abbate, I. B. Bhat, and P. Das, Appl. Phys. Lett. **60**, 862 (1992).
[8] R. Nicolini, L. Vanzetti, Guido Mula, G. Bratina, L. Sorba, A. Franciosi, M. Peressi, S. Baroni, R. Resta, A. Baldereschi, J. E. Angelo, and W. W. Gerberich, Phys. Rev. Lett. **72**, 294 (1994).
[9] Y. H. Wu, T. Toyoda, Y. Kawakami, and S. Fujita, Jpn. J. Appl. Phys., Part 2 **29**, 144 (1990).